DEVELOPMENT AND FIRST BEAM OBSERVATIONS OF AN ULTRA-FAST BUNCH-BY-BUNCH X-RAY BEAM SIZE MONITOR AT SuperKEKB

R. Nomaru[†,1,2], G. Mitsuka[2], M. Andrew[3], K. Yoshihara[3], C. Driver[3]
[1]The University of Tokyo, Tokyo, Japan
[2]High Energy Accelerator Research Organization, Ibaraki, Japan
[3]University of Hawaii, HI, USA

Abstract

We have developed a new ultra-fast bunch-by-bunch beam size monitor for SuperKEKB and initiated beam observations in the electron ring (HER) starting in November 2025. Using this system, we successfully acquired data and achieved, for the first time at SuperKEKB, bunch-by-bunch measurements of the beam size. The measured beam sizes show good agreement with those obtained using the conventional, slower beam size monitor, demonstrating the reliability of the new system. The high temporal resolution of the monitor enables detailed investigation of beam size variations along the bunch train. Furthermore, the measurements reveal that the bunch-to-bunch beam size variation increases during collision operation compared to single-beam conditions, suggesting a significant contribution from beam–beam effects.

INTRODUCTION

The SuperKEKB accelerator [1] is a high-luminosity electron–positron collider operating with 7 GeV electrons and 4 GeV positrons. In March 2026, it achieved a peak luminosity of 5.2×10^{34} $\mathrm{cm^{-2}s^{-1}}$ surpassing its previous world record. Commissioning efforts are ongoing toward even higher luminosity. In such high-luminosity colliders, it is crucial to stably store a large number of high-current bunches in the storage rings. Under these conditions, various beam instabilities—such as electron cloud effects, ion trapping, and beam–beam interactions—can degrade machine performance. Understanding these effects requires diagnostics with high temporal resolution capable of resolving individual bunches.

To address this need, we have developed a new bunch-by-bunch beam size monitor for SuperKEKB. This system combines synchrotron radiation X-rays with a silicon strip detector, enabling fast sampling of beam images. During the 2025–2026 operation periods, we successfully performed the first bunch-by-bunch beam size measurements using this system. In this paper, we describe the detector system, measurement methodology, data analysis procedures, and present initial beam measurement results.

BUNCH-BY-BUNCH X-RAY BEAM SIZE MONITOR

At SuperKEKB, the beam size is measured using synchrotron radiation X-rays emitted from bending magnets. The X-rays pass through a coded aperture mask, and the resulting image is reconstructed and fitted to extract the beam size [2]. In routine operation, a CMOS camera is used as the imaging device. While this system has been extensively used during commissioning, its exposure time (typically tens of microseconds or longer) and limited frame rate (<100 Hz) prevent bunch-by-bunch measurements. To overcome this limitation, we developed a new detector system, referred to as the Silicon X-ray Radiation Monitor (SiXRM), which employs a silicon strip sensor instead of a CMOS camera for high-speed sampling, thereby enabling bunch-resolved measurements. This system is designed to complement the conventional CMOS-based monitor, providing time-resolved information that is not accessible with the existing system.

Figure 1 shows the SiXRM system. It consists of a silicon sensor board, a preamplifier board, and a data acquisition (DAQ) board. The system was developed in collaboration between KEK, the University of Hawaii, and SLAC National Accelerator Laboratory, and the DAQ is based on the system used in the Belle II TOP detector [3]. The silicon strip sensor has 128 strips in the vertical direction, making the system sensitive to the vertical beam size. Due to wire-bonding issues between the sensor and readout electronics, currently only 42 channels are used. The DAQ system uses waveform sampling ASICs and FPGAs, enabling analog waveform sampling at 2.7 GSa/s followed by subsequent digitization. Given the minimum bunch spacing of 4 ns in the SuperKEKB main ring, this sampling rate is sufficient for bunch-by-bunch measurements. A more detailed description of the system design and its commissioning can be found in Ref. [4]. The waveform length per acquisition is limited to approximately 12 RF buckets (~24 ns). A full-turn measurement (~10 μs, 5120 buckets) is therefore obtained by repeatedly acquiring short waveform windows while shifting the acquisition timing. The full waveform is reconstructed by concatenating these segments. Each window acquisition takes about 50 ms, and a full-turn measurement requires approximately 20 seconds.

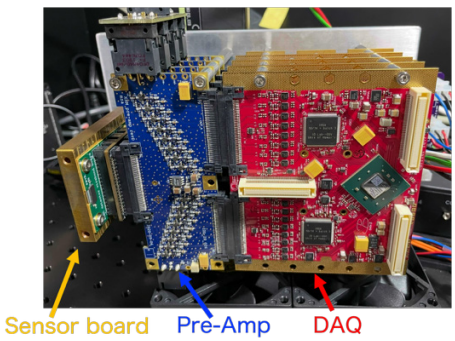

Figure 1: Photograph of the SiXRM system.

† nomaru@post.kek.jp

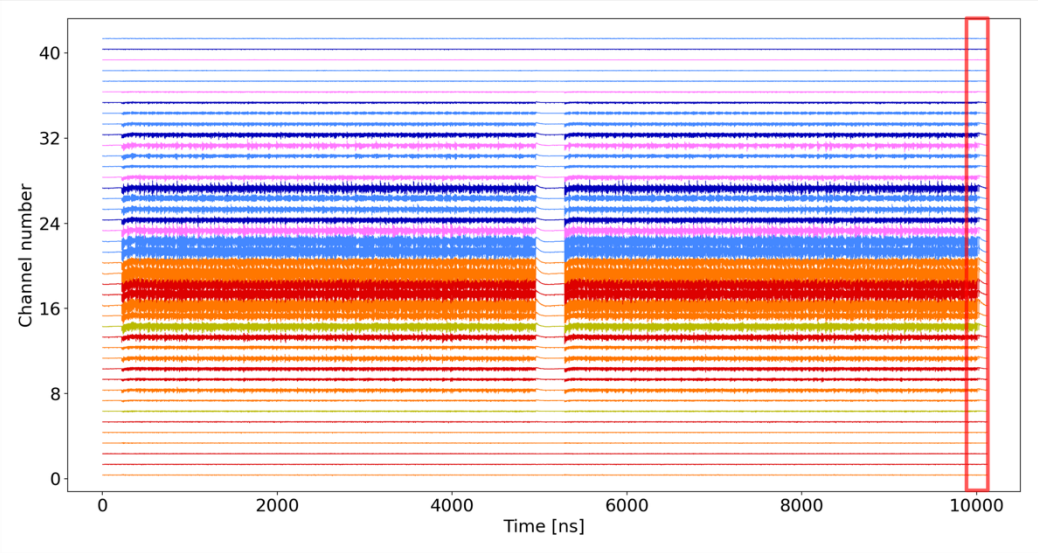

Figure 2: Beam observation in the HER using the SiXRM. The measurement was performed at 2026-02-02 09:02:48, with a beam current of 800 mA.

BEAM OBSERVATION AND ANALYSIS

Raw Waveform Observation

Beam observations using the SiXRM were performed in the electron ring (HER) starting from the operation period in November 2025. Figure 2 shows an example of a measurement result. The plot displays waveforms from each channel (0–41) of the silicon strip sensor arranged vertically. The horizontal axis represents one full turn (~10 μs), and the waveforms of all bunches within one turn are shown. As described in the previous section, this waveform is constructed by concatenating multiple short waveforms of 12 RF buckets. Therefore, it should be noted that this is not a waveform obtained in a single turn. Regions without waveforms are observed at both ends and in the middle of the plot; these correspond to gaps required for the rise time of the abort kicker power supply during beam abort. The presence of two gaps and two bunch trains is clearly visible, confirming that the system successfully records the full-turn information. Figure 3 shows an enlarged view of the red boxed region on the right side of Fig. 2. Numerous downward pulses are observed in each channel waveform, and each pulse corresponds to a single bunch. By calculating the height of each pulse and arranging them along the channel direction, an X-ray image formed by the coded aperture is expected to be reconstructed.

Pulse Height Extraction

As seen in Fig. 3, each pulse is followed by overshoot and ringing. To accurately determine the pulse height under such conditions, the following procedure is adopted:

- 1. Reference channel selection
  One channel (typically ch18) near the center with a large signal amplitude is chosen as a reference channel.
- 2. Spline interpolation
  Waveforms are smoothed using cubic spline interpolation.

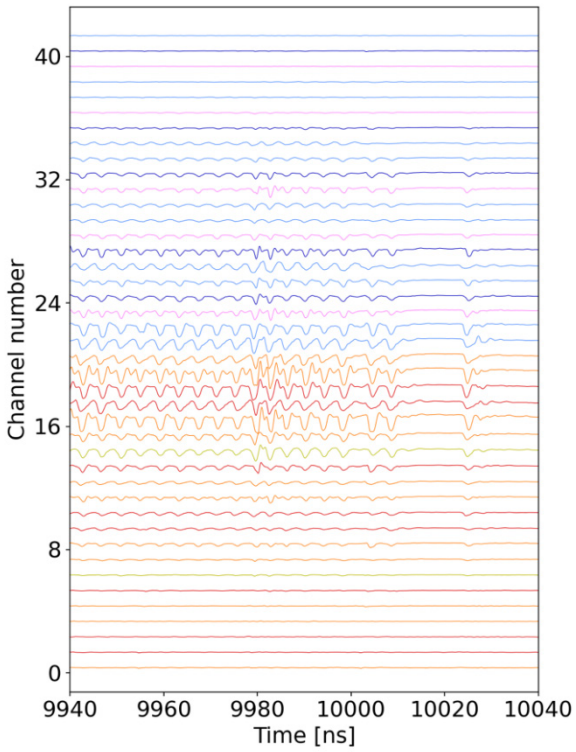

Figure 3: Enlarged view of the red boxed region on the right side of Fig. 2.

- 3. Fine timing Alignment
  Since the timing of waveforms may slightly differ between channels, each waveform is shifted within ±1 ns to maximize correlation with the reference channel.
- 4. Peak detection
  Peaks are identified in the reference channel using the `find_peaks` function from SciPy [5]. These peak timings are applied to all channels.

- 5. Peak windowing
  For each detected peak (i.e., each bunch), a ±2.5 ns window is defined. The minimum value within this window (since pulses are negative) is taken as the peak value for each pulse.
- 6. Baseline determination
  Figure 4 schematically illustrates the baseline determination method. Within the same ±2.5 ns window, the maximum value in the right half (green region in Fig. 4) and that in the left half (orange region) are identified (green and orange markers, respectively). The midpoint of the line connecting these two points (black marker) is defined as the baseline.
- 7. Pulse height calculation and calibration
  The pulse height is defined as the difference between the peak value and the baseline, as indicated by the pink arrow in Fig. 4. Calibration factors for each channel are then applied. These calibration factors are obtained using a test bench with pulsed laser illumination (see Ref. [4] for details).

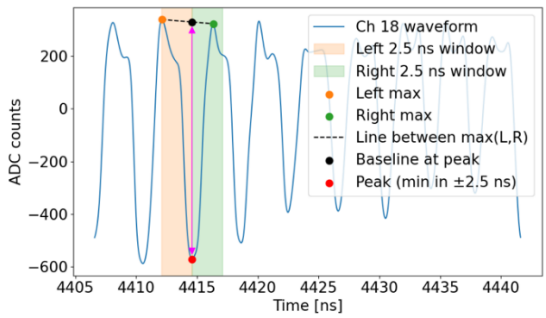

Figure 4: Schematic illustration of the pulse baseline and height extraction method. A single pulse in channel 18 from the measurement shown in Fig. 2 is used as an example.

Image Reconstruction and Fitting

After extracting the pulse heights, the X-ray image for each bunch is obtained by arranging the pulse heights along the channel direction. Figure 5 shows a heatmap obtained by reconstructing the X-ray image for each bunch from the pulse heights and superimposing all bunch images. The horizontal axis represents the channel number (0–41), the vertical axis represents pulse height, and the color indicates the number of bunches in each bin. A characteristic coded aperture image profile is clearly observed (see Ref. [2] for reference).

The next step is to fit the image for each bunch to extract the beam size. The fitting method and templates are essentially the same as those used in the CMOS camera system [2]. The following six parameters are used in a least-squares fit:

- μ : vertical beam position
- σ : vertical bem size
- v_{offset} : vertical image offset
- x_0 : horizontal image offset
- norm : vertical image scaling factor
- scale : horizontal image scaling factor

Templates corresponding to various μ and σ values are prepared in advance and used for fitting.

Figure 6 shows the fitted beam sizes for all bunches in the measurement of Fig. 2. The horizontal axis is the same as in Fig. 2, and the vertical axis shows the fitted σ, i.e., the vertical beam size. Each point corresponds to one bunch. The average beam size over all bunches in this measurement was 54.3 μm. At the same time, the beam size measured by the CMOS camera was 56.6 μm, showing good agreement with the SiXRM result. As an example of the fitting, Fig. 7 shows the fit for a single bunch, demonstrating that the fitting works well.

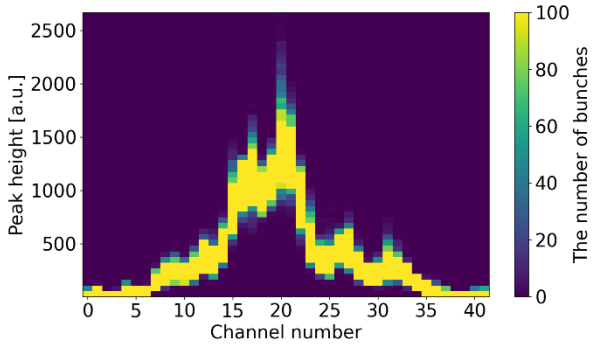

Figure 5: Heatmap obtained by reconstructing the X-ray image for each bunch from the pulse heights and superimposing all bunch images for the measurement shown in Fig. 2.

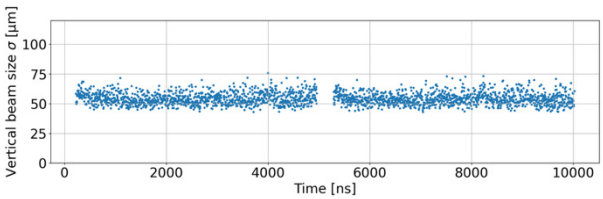

Figure 6: Fitted vertical beam size (σ) for all bunches in the measurement shown in Fig. 2.

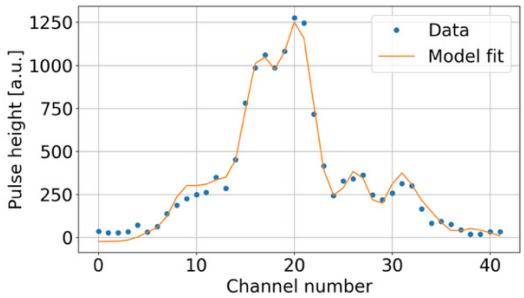

Figure 7: Example of the X-ray image fitting for a single bunch in the measurement shown in Fig. 2.

COMPARISON BETWEEN SIXRM AND CMOS CAMERA

To evaluate the reliability of the SiXRM measurements, we compared them with those obtained using the well-established CMOS camera-based beam size monitor. For this comparison, we used 2429 HER measurements acquired

between November 30, 2025, and February 4, 2026, covering a wide range of machine conditions and beam sizes. Here, one measurement corresponds to a full-turn measurement, as shown in Fig. 2. Figure 8 shows the comparison between the beam sizes measured by the SiXRM and those measured simultaneously by the CMOS camera. The horizontal axis shows the beam size measured by the CMOS camera, while the vertical axis shows the beam size averaged over all bunches in one turn as measured by the SiXRM. The error bars represent the standard deviation of the bunch-by-bunch beam sizes within the turn measured by the SiXRM. Each point corresponds to one full-turn measurement. The diagonal dashed line indicates perfect agreement between the two systems. Most of the data points are distributed close to this line, demonstrating that the SiXRM provides reliable beam size measurements.

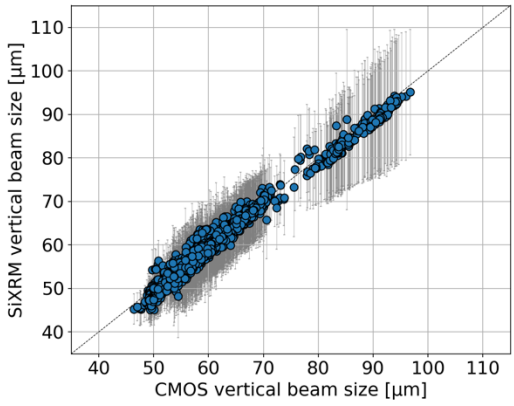

Figure 8: Comparison of beam size measurements between the SiXRM and the CMOS camera-based beam size monitor.

BEAM SIZE VARIATION WITHIN THE BUNCH TRAIN

In this section, we present several interesting results obtained from the analysis of data acquired with the SiXRM. A clear difference is observed between collision operation and single-beam operation. Figure 9 shows a time-series plot of the machine operation at a specific period. The horizontal axis represents time, and the beam currents and beam sizes of the electron ring (HER) and the positron ring (LER) measured by the CMOS camera are plotted. Around 10:06, only the LER beam was aborted, after which the machine transitioned to HER single-beam operation. Beam size measurements of the HER using the SiXRM were performed at 10:00:02 (during collision operation, indicated by a magenta vertical dashed line in Fig. 9) and at 10:07:49 (after the LER beam abort, i.e., during HER single-beam operation, also indicated by a black vertical dashed line). The corresponding results are shown in Figs. 10 and 11. A comparison of these results shows that the bunch-to-bunch variation of the beam size within the train is larger during collision operation than during single-beam operation (as indicated by the larger spread marked by the red arrows in the figures). This suggests that the beam–beam interaction enhances the variation of the beam size within the bunch train.

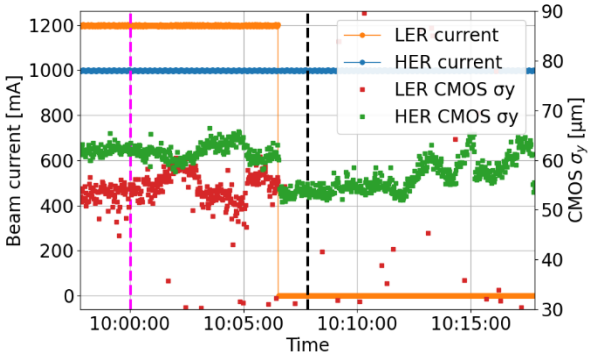

Figure 9: Time-series plot of accelerator operation on February 3, 2026, showing the beam currents and beam sizes recorded by the CMOS camera in the HER and LER.

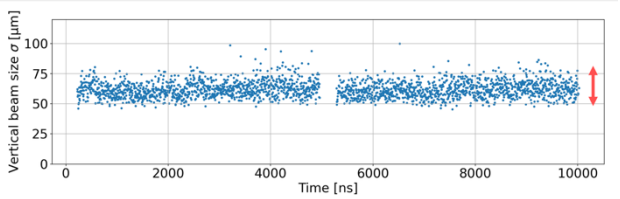

Figure 10: Bunch-by-bunch beam size in the HER measured by the SiXRM at 10:00:02 on February 3, 2026, during collision operation.

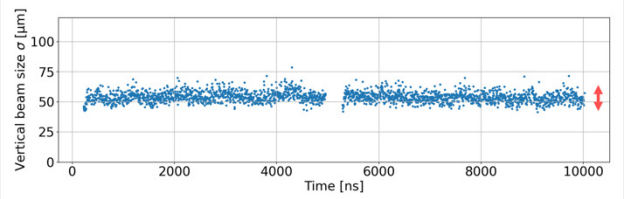

Figure 11: Bunch-by-bunch beam size in the HER measured by the SiXRM at 10:07:49 on February 3, 2026, during single-beam operation.

To quantify this effect, we focus on this variation and evaluate it using the standard deviation of the beam size over all bunches within one turn. Hereafter, this quantity is referred to as the beam size variation. Figure 12 shows a scatter plot of the beam size variation versus the HER average beam size measured simultaneously by the CMOS camera. The dataset used in this plot consists of 6177 measurements taken during collision operation between January 27 and February 15, 2026, with HER beam current greater than 700 mA. The color scale represents the specific luminosity. From this plot, a positive correlation between the beam size variation and the HER average beam size is observed. This indicates that when the beam size increases during collision operation, the beam size of each bunch in the train do not uniformly become larger; instead, the beam size increases while the bunch-to-bunch variation simultaneously broadens. This provides the first clear evidence of such a behavior. Furthermore, by examining the color scale, it is found that even at the same average beam size (i.e., at

a fixed value on the vertical axis), a smaller beam size variation corresponds to higher specific luminosity. This suggests that not only the increase in the average beam size but also the beam size variation contributes to the change in luminosity. Figure 13 shows a scatter plot of the beam size variation versus the specific luminosity, with the color indicating the HER beam current. A negative correlation between the beam size variation and the specific luminosity is observed, suggesting that the beam size variation is related to luminosity performance.

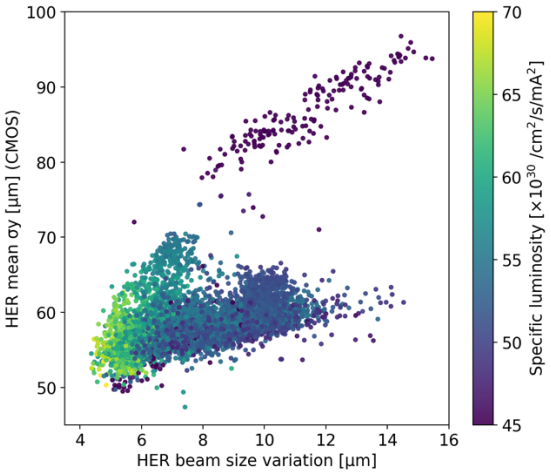

Figure 12: Relationship between the beam size variation and the HER beam size measured by the CMOS camera. The color scale represents the specific luminosity.

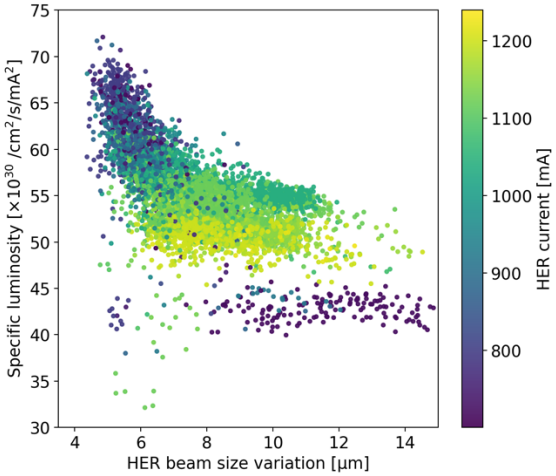

Figure 13: Relationship between the beam size variation and the specific luminosity. The color scale represents the HER beam current.

CONCLUSION AND OUTLOOK

We have developed a new ultra-fast beam size monitor for SuperKEKB and successfully performed bunch-by-bunch beam size measurements for the first time in the electron ring. The reliability of this new monitor has been confirmed through comparison with the existing system. In the future, we plan to improve the readout electronics to overcome current limitations, such as the short acquisition window, and to install the system in the positron ring as well. Analysis of the measured data suggests that beam–beam interactions may induce bunch-to-bunch variation of the beam size within the train, and that this variation is correlated with the luminosity. Further studies, including simulations and combined analysis with other diagnostics, are planned to deepen the understanding of this phenomenon.

REFERENCES

[1] SuperKEKB Design Report, https://kds.kek.jp/event/15914/

[2] E. Mulyani, J. W. Flanagan, M. Tobiyama, H. Fukuma, H. Ikeda, and G. Mitsuka, "First measurements of the vertical beam size with an X-ray beam size monitor in SuperKEKB rings," *Nucl. Instrum. Methods Phys. Res., Sect. A*, vol. 919, pp. 1–15, Mar. 2019. doi:10.1016/j.nima.2018.11.116

[3] M. Andrew, "128 channel waveform sampling digitizer/readout in the TOP counter for the Belle II upgrade," in *Technology and Instrumentation in Particle Physics 2014*, Ed., in TIPP2014. Sissa Medialab, Jul. 2015, p. 171. doi:10.22323/1.213.0171

[4] R. Nomaru, G. Mitsuka, M. Andrew, K. Yoshihara, C. Driver, and L. Ruckman, "R&D of an ultrafast X-ray beam size monitor for SuperKEKB", in *Proc. IBIC'25*, Liverpool, UK, Sep. 2025, pp. 435-439. doi:10.18429/JACoW-IBIC2025-TUPCO31

[5] find_peaks — SciPy v1.17.0 Manual https://docs.scipy.org/doc/scipy/reference/generated/scipy.signal.find_peaks.html